Fluid Phase Equilibria 498 (2019) 9–22

Contents lists available at ScienceDirect

Fluid Phase Equilibria

journal homepage: www.elsevier.com/locate/fluid

Correlation and prediction of thermodynamic properties of dilute solutes in water up to high *T* and *P*. I. Simple fluids He, Ne, Ar, Kr, Xe, Rn, H_2, N_2, O_2, CO, CH_4

Andrey V. Plyasunov [a, *], Valentina S. Korzhinskaya [a], John P. O'Connell [b, c]

[a] Institute of Experimental Mineralogy, Russian Academy of Sciences, Chernogolovka, Moscow Region, 142432, Russia
[b] University of Virginia, Charlottesville, VA, 22904, USA
[c] California Polytechnic State University, San Luis Obispo, CA, 93407, USA

ARTICLE INFO

Article history:
Received 27 March 2019
Received in revised form
5 June 2019
Accepted 12 June 2019
Available online 17 June 2019

Keywords:
Thermodynamic properties
Aqueous mixtures of simple fluids
Krichevskii parameter
Henry's constant
Infinite-dilution fugacity coefficient

ABSTRACT

Fugacity coefficients of dilute aqueous solutions of six noble gases and five simple fluids have been correlated from ambient conditions (298 K, 0.1 MPa) to high temperatures (up to 2000 K) and water densities as high as 1500 kg m^{-3}. A correlation is developed for the function, $A_{12}^{\infty} = V_2^{\infty}/\kappa_T RT$, that includes known constraints: second virial coefficients at low-water densities, rigid-body behavior at high-water densities, near-critical principles, and corresponding-states relations. Reasonable agreement with an extensive, evaluated database of volumetric and solubility measurements has been achieved over the entire range of conditions, though comparisons of calculated with recommended Henry's constants suggest reconsiderations of recommendations for He and CO at temperatures above 550 K.

© 2019 Elsevier B.V. All rights reserved.

1. Introduction

Thermodynamic properties of components of aqueous solutions at high temperatures and pressures are necessary for both technological applications and for geochemical modeling of water-gas-rock interactions. The Helgeson–Kirkham–Flowers (HKF) model is often used to calculate the Gibbs energies and other thermodynamic functions at infinite dilution in water of ions [1,2] and neutral solutes [3] at high *T* and *P*. The *T*-*P* range of applicability for this model was recently [4] extended to ~1500 K and 6 GPa. Application of the model to neutral (noncharged) species had a limited theoretical basis and was later shown unable to quantitatively reproduce available data at near-critical and supercritical temperatures [5–10]. Equations of state (EoS), with parameter mixing rules in the geochemical literature are more successful at predicting thermodynamic properties, including infinite-dilution fugacity coefficients, ϕ_2^{∞}, (related to Gibbs energies) of dissolved aqueous gases up to very high *T* and *P*. These include models from molecular simulation-based *PVTx* properties of binary water-gas systems [11,12], from perturbation theory [13], and others. Several literature EoS have been coded by R.J. Bakker [14] and may be freely downloaded from: http://fluids.unileoben.ac.at/Computer.html. Our analyses [9,10,15] show general agreement of results of these EoS up to water densities of ~1000 kg m^{-3}, although the differences significantly increase - up to ~3 $\log_{10}$ units - at pressures in excess of 5–6 GPa. Since these EoS are intended for the use at supercritical temperatures, their applications at subcritical temperatures, reported mostly as Henry's constants, k_H, are problematic. In addition, such "classical" EoS cannot accurately describe properties in the near-critical region where long-range density and composition fluctuations arise [16]. These issues suggest developing property models from alternative concepts.

One approach is to model derivative partial molar properties, particularly the partial molar volume, V_2^{∞}, and use thermodynamic manipulations to establish expressions for partial molar heat capacities, $C_{p,2}^{\infty}$, and k_H [8,17,18]. The basis for this was suggested in Ref. [7]. These models closely reproduce precise V_2^{∞} results over the whole temperature range of measurements, from 298.15 up to 720 K, at pressures up to 40 MPa. It has been recently shown that early formulations are less reliable for extrapolation to higher temperatures and densities/pressures [9,15]. A method consistent with known theoretical constraints (at low water densities, at high

* Corresponding author.
E-mail address: andrey.plyasunov@gmail.com (A.V. Plyasunov).

https://doi.org/10.1016/j.fluid.2019.06.012
0378-3812/© 2019 Elsevier B.V. All rights reserved.

water densities, and at the critical point of water) was proposed [9]. Using limited ambient condition data, the method was applied to ϕ_2^∞ at 1000 and 2000 K for CO_2, and at 1000 K for nonpolar CH_4 and polar substances H_2S, SO_2, and NH_3.

The goal of the present project is to systematically generalize the method of [9] for describing aqueous infinite-dilution fugacity coefficients over wide temperature and pressure ranges. The present work treats simple fluids, that is the noble gases (He, Ne, Ar, Kr, Xe, Rn), and compounds that are nearly spherical with dipole moments equal to or near zero (H_2, N_2, O_2, CO, CH_4).

The method treats both water and solutes as non-ionized species which places limits on the conditions of application. Both high temperature [19] and high pressure [20] cause dissociation and decomposition of water. Therefore, the upper temperature limit has been chosen as 2000 K, based on an *ab initio* investigation [19] of the H_2O–H_2 mixture that concluded "at 2000 K and below the mixture is almost fully molecular", though significant dissociation occurs at higher temperatures. The upper limit for the water density, ρ_1^*, is taken as 1500 kg m^{-3}. While somewhat arbitrary, this limit is supported by the experimental observation that "at lower pressure (below approximately 12 GPa) liquid water has a predominantly molecular character" [20]. The corresponding maximum pressures increase from ~5.3 GPa at 500 K to ~7.7 GPa at 1000 K to ~9.7 GPa at 1500 K and to ~11.4 GPa at 2000 K. At temperatures below 500 K, the maximum ρ_1^* is determined by the *PT* coordinates of the melting curve of ice [21]. It increases from ~1250 kg m^{-3} at 300 K to ~1350 kg m^{-3} at 350 K and to ~1450 kg m^{-3} at 475 K. We also set a lower temperature limit of 298.15 K for applying the approach, as discussed below.

The work is organized as follows: first, we give Eq. (1) for calculating the fugacity coefficients of an infinitely dilute solute in water, ϕ_2^∞, through the density integration of the function A_{12}^∞ defined in Eq. (2). As discussed previously [9], the values of A_{12}^∞ for many classes of neutral solutes can reliably be estimated over wide ranges of temperature (298–2000 K) and water density (0–1500 kg m^{-3}). The systematic application of such estimation methods to simple fluids is discussed in Section 2. In Section 3, the generated values of A_{12}^∞ (298–2000 K, 0–1500 kg m^{-3}) for each of the eleven solutes under consideration were fitted with Eq. (18), with correlated fugacity coefficients compared with literature data at supercritical (Section 3.2) and subcritical (Section 3.3) temperatures.

2. Theory

2.1. Fundamental relations

Since the proposed method for predicting thermodynamic properties of nonelectrolytes at infinite dilution in water has been thoroughly explained [9,10,15], only a brief outline will be given here. The basic equation for the calculation of ϕ_2^∞ is an isothermal integration over density of the function A_{12}^∞ [7].

$$\ln \phi_2^\infty = \int_o^{\rho_1^*} (A_{12}^\infty - 1)\frac{d\rho_1^*}{\rho_1^*} - \ln\frac{PV_1^*}{RT} \tag{1}$$

where

$$A_{12}^\infty = V_2^\infty/\kappa_T RT \tag{2}$$

with $\kappa_T = 1/\rho_1^*(\partial\rho_1^*/\partial P)_T$, the isothermal compressibility of pure solvent. Here, the subscript *2* refers to the solute and *1* to the solvent. Note that here and below ρ_1^* is in kg m^{-3} and V_1^* (the molar volume of pure water) and V_2^∞ are in cm^3 mol^{-1}. The superscript ∞ denotes a property at infinite dilution, and * a pure-component property. The dimensionless quantity, A_{12}^∞, is linearly related to the spatial integral of the molecular solute-water direct correlation function at infinite dilution [7] arising in Fluctuation Solution Theory [22,23]. Theoretically, A_{12}^∞ is a smooth, continuous, and finite function at all conditions, including at the pure-solvent critical point, where the derivatives of the standard chemical potential of a solute diverge [24,25]. The critical A_{12}^∞ is finite with a value that depends on the components [26] because the divergent V_2^∞ is in the numerator and the divergent κ_T is in the denominator. For an ideal gas (IG), $A_{12}^\infty = 1$.

The current method predicts A_{12}^∞ values at different temperatures and water densities, considering theoretical constraints wherever possible [9,15]. The initial departures from IG are linear in density

$$A_{12}^\infty = 1 + 2\rho_1^* B_{12} + \ldots \tag{3}$$

where B_{12} is the temperature-dependent water-solute cross second virial coefficient [27,28]. At densities below ~950 kg m^{-3}, A_{12}^∞ is not a strong function of temperature [7]. At densities above ~950 kg m^{-3} at ambient temperatures and above ~450 kg m^{-3} at more than 1500 K, V_2^∞ and, correspondingly, A_{12}^∞, can be predicted [9,15,29] on the basis of the theory of mixture of hard spheres that depends only on density [30]. An experimental value of V_2^∞ at the standard state of 298.15 K and 0.1 MPa is needed to predict A_{12}^∞ at high water densities. At the critical point of water, A_{12}^∞ can be calculated from the value of the Krichevskii parameter [24], which is either known [31] or can be estimated [32] for many gases in water. References [24,25] define the Krichevskii parameter as the derivative $(\partial P/\partial x)^c_{V,T,x=0}$, at the critical point of a solvent. The Krichevskii parameter governs all the thermodynamic properties of dilute solutions in the neighborhood of the solvent critical point. At intermediate water densities, $500 < \rho_1^* < 900$ kg m^{-3}, a variant of the corresponding-states principle was proposed for estimating A_{12}^∞ [9,29]. After values of A_{12}^∞ are available over the whole range of density, Equation (1) can be used to obtain ϕ_2^∞. The variation of A_{12}^∞ is nonmonotonic at lower temperatures (<293 K) and pressures [29]. Though the observed low-temperature maximum disappears at pressures in excess of ~100 MPa, since our main interest is in high-temperature behavior, we concluded that accounting for this behavior would not be worthwhile. Thus, the low temperature limit of the correlation was set as 298.15 K.

2.2. Application to simple fluids

2.2.1. Second cross virial coefficients

Variations of B_{12} with T for interactions of water with many simple fluids (He, Ne, Ar, H_2, N_2, O_2, CO, CH_4) have been determined from accurate *ab initio* intermolecular potentials and available experimental data [33–39]. Such data have been fitted using polynomials of the type

$$B_{12}(T) = \sum_{i=1}^{4} a_i \left(\frac{T}{100}\right)^{b_i} \tag{4}$$

Parameters of Equation (4) for various simple fluids are given in Table 1. For water interactions with Kr, Xe, and Rn, values of B_{12} have been estimated as described in Ref. [40] and fitted with Equation (4). For CH_4–H_2O interactions, accurate B_{12} values are recommended in Ref. [36] up to 1000 K, these results were extrapolated to 2000 K by the method of [40] and fitted with Equation (4). The empirical method [40] is based on the application of the Tsonopoulos corresponding-states correlation [51] to 29 binary aqueous gas-water systems, which included nonpolar

Table 1
Parameters of Equation (4) for calculating B_{12} in cm^3 mol^{-1}. The a_i are in cm^3 mol^{-1}.

Gas	He [a]		Ne [b]		Ar [b]		Kr [c]		Xe [c]		Rn [c]	
i	a_i	b_i	a_i	b_i	a_i	b_i	a_i	b_i	a_i	b_i	a_i	b_i
1	55.57	−0.347	45.8586	−0.30	96.1591	−0.31	308.36	−0.2	87.847	−0.1	101.91	−0.1
2	−59.25	−0.85	59.4400	−0.48	−211.074	−0.82	−333.91	−0.3	−182.245	−0.6	−235.28	−0.6
3	13.32	−1.45	−121.583	−0.69	−96.4425	−2.24	−408.10	−1.6	−659.674	−1.8	−1049.8	−1.9
4	−4.767	−2.1	−12.5141	−2.14	−12.6006	−4.60	−460.68	−3.5	−909.213	−3.8	−1571.9	−4.0

Gas	H_2 [d]		N_2 [e]		O_2 [f]		CO [g]		CH_4 [h]	
i	a_i	b_i	a_i	b_i	a_i	b_i	a_i	b_i	a_i	b_i
1	33.047	−0.21	67.595	−0.24	124.605	−0.33	493.709	−0.45	109.22	−0.2
2	−250.41	−1.50	−249.83	−1.06	−214.421	−0.73	−579.466	−0.57	−202.52	−0.6
3	285.42	−2.26	−204.38	−3.22	−102.818	−2.03	−248.146	−2.00	−235.86	−2.0
4	−186.78	−3.21	0	0	−22.360	−4.07	−271.885	−4.25	−297.63	−3.0

[a] [33].
[b] [34].
[c] – our fit of B_{12} values estimated as described in Ref. [40].
[d] [35].
[e] [37].
[f] [38].
[g] [39].
[h] Our fit of B_{12} at 298–1000 K [36] and at 1000–2000 K estimated as described in Ref. [40].

compounds (Ar, C_2H_4, *n*-alkanes up to *n*-octane, etc.), polar (CH_3Cl, HCl as examples) and hydrogen bonded compounds (alcohols, ammonia). It was shown that the mixture-specific parameter of Tsonopoulos correlation, k_{12}, after a small "size" correction, depends linearly on the Gibbs energy of hydration (Henry's constant in water) of a compound at 298 K and 0.1 MPa. The method [40] is used to estimate B_{12} for aqueous mixtures in the absence of experimental data.

2.2.2. *Infinite-dilution partial molar volumes of simple fluids in water at 298.15 K*

Based on the theory of mixtures of hard spheres [30], values V_2^∞ for simple fluids in water at $T_r = 298.15$ K and $P_r = 0.1$ MPa can be used [9,29] to calculate thermodynamic properties at high water densities: at $\rho_1^* > 950$ at 400 K, $\rho_1^* > 900$ at 1000 K, and at $\rho_1^* > 450$ for $T \geq 1500$ K with the relation below

$$V_2^\infty(T,P) = V_2^\infty(T_r,P_r)\frac{\rho_1^*(T_r,P_r)}{\rho_1^*(T,P)} \quad (5)$$

All simple fluids are very poorly soluble in water at ambient conditions. As a consequence, V_2^∞ values [41–49] of most of these gases in water at 298.15 K are known with significant uncertainties. For example, the V_2^∞ data [49] at 298.15 and 303.15 K differs up to 4 cm^3 mol^{-1} (for O_2, Ar) and even 6 cm^3 mol^{-1} (for CH_4). The effects of the small temperature dependence of 298 and 303 K are unlikely to explain the differences, so they must arise from experimental error. In addition, the only experimental data point for Kr in water [44] is surprisingly close to V_2^∞ of argon. Also, the data points for Xe [48] may be affected by formation of clathrates at the 33.4 MPa pressure of the measurements. Finally, no data are reported for Ne and Rn. The lack of complete measurements has required developing empirical estimates of V_2^∞ for a number of simple fluids in water at 298.15 K and 0.1 MPa, as described below.

The reported results for Ar, H_2, N_2, O_2, CO, and CH_4, for which there are consistent values from various research groups, were accepted. Also accepted, although with a larger uncertainty, was the reported value for He [49].

Several relations to correlate V_2^∞ in water at 298.15 K and 0.1 MPa have been proposed in the literature. According to the corresponding-states principle (CSP) [50,51], results of V_2^∞/V_c vs. T/T_c for simple fluids should lie on a single curve, while variations for other solute families will be different. As discussed in Ref. [44], V_2^∞ varies approximately linearly with V_c, the critical volume of the pure solute. Fig. 1a confirms that observation with:

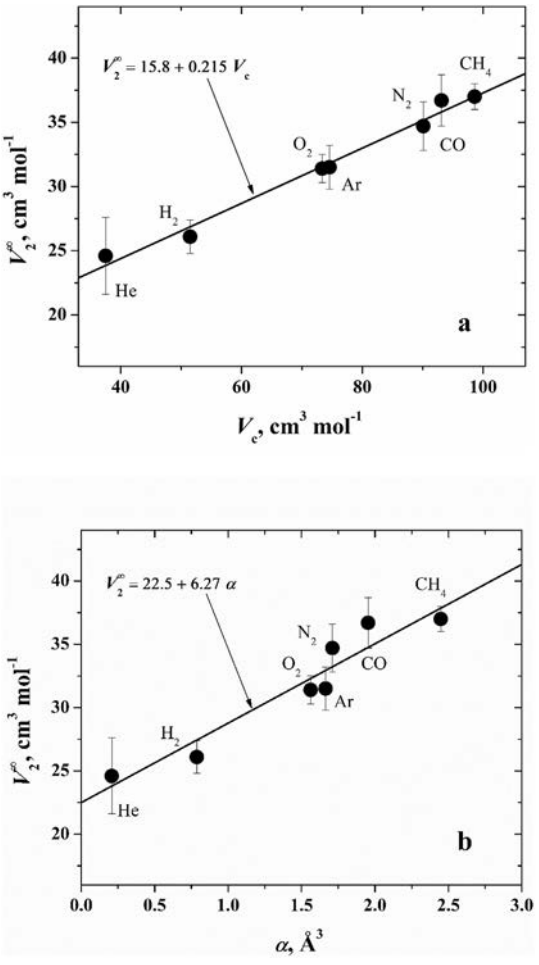

Fig. 1. Linear correlations of V_2^∞ for simple fluids in water with a) V_c, critical volumes of pure gases, and with b) α, molecular polarizability of gases.

$$V_2^{\infty} = 15.8 + 0.215V_c \quad (6)$$

when all values are in $cm^3\ mol^{-1}$. Note that for "quantum gases" He, Ne, and H_2 the so-called "classical" values of V_c have been used, as recommended for corresponding-states relations [51].

A correlation between V_2^{∞} and the molecular polarizability of a solute, α, has been suggested [52]. Fig. 1b indicates that relation is approximately linear:

$$V_2^{\infty} = 22.5 + 6.27\alpha \quad (7)$$

where the molecular polarizability is given in $Å^3$ units.

The concept of an empty layer of thickness δ_{sph} devoid of water around a spherical nonpolar solute of van der Waals radius of r_{vdW} suggests the following approximation (*e.g.*, [30], [53])

$$V_2^{\infty} = \frac{4\pi}{3}\left(r_{vdW} + \delta_{sph}\right)^3 \quad (8)$$

The theory for mixtures of hard spheres [30] predicts that for small r_{vdW}, δ_{sph} is large and decreasing, converging to a constant value at large r_{vdW}. Fig. 2a confirms this behavior; among the several relations that equally well approximate the data, Equation (9) has been selected:

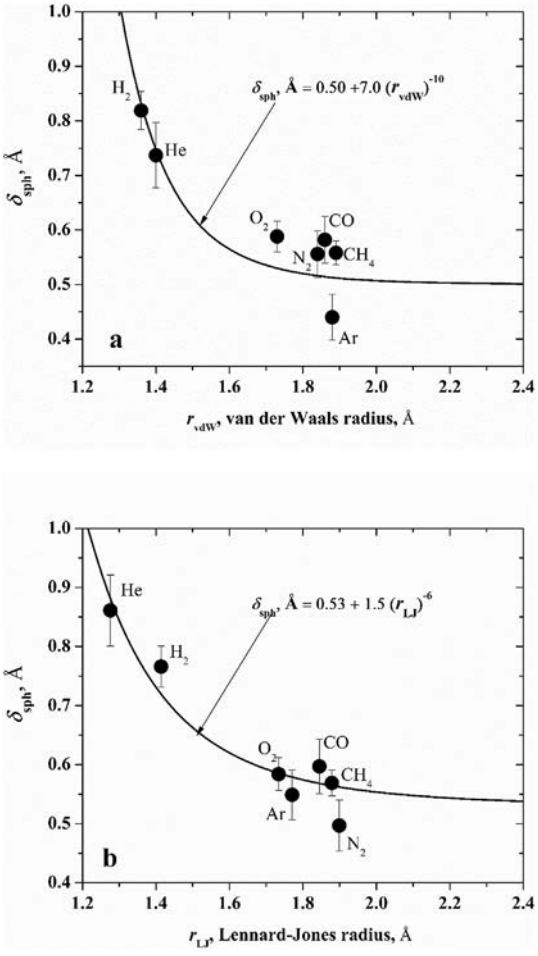

Fig. 2. Evaluation of δ_{sph}, the solute-solvent border thickness, from correlation of V_2^{∞} with the van der Waals (a) or Lennard-Jones (b) radii of solutes.

$$\delta_{sph} = 0.50 + 7.0(r_{vdW})^{-10} \quad (9)$$

where both δ_{sph} and r_{vdW} are given in Å units. The necessary values of r_{vdW} are taken from Refs. [54,55]. A final proposed measure of molecular size in solution is the radius given by the Lennard-Jones intermolecular potential model, r_{LJ}. Our correlation for this form is

$$\delta_{sph} = 0.53 + 1.50(r_{LJ})^{-6} \quad (10)$$

where both δ_{sph} and r_{LJ} are given in Å units.

The results from all of these models are presented in Table 2. No compelling argument favors one method over the others, so all proposed relations have been employed as listed in the ninth column of Table 2. The average of values from Equations (7) to 10), listed in the tenth column of Table 2, have been used in subsequent calculations.

2.2.3. Values of the Krichevskii parameter and vapor-liquid distribution coefficients of simple fluids in water

Values of the A_{12}^{∞} at the critical point of water can be calculated with the relation [56]:

$$A_{12}^{\infty}\left(T_c, \rho_{1,c}^*\right) = A_{Kr}\frac{V_{1,c}^*}{RT_c} \quad (11)$$

where $V_{1,c}^*$ is the critical molar volume of water, and A_{Kr} is the (constant) Krichevskii parameter [24,57]. For most simple fluids in water, values of A_{Kr} are known with high precision [31], mainly from high-temperature values of solute distribution between equilibrium vapor and liquid phases of water [58].

The distribution coefficient is defined as $K_D = \lim_{x,y\to 0} y/x$, where y and x are the mole fractions of solute in the coexisting vapor and liquid phases, respectively. At the solvent's critical point, where both phases are identical, K_D is unity. Expanding the chemical potential of a solute about the solvent's critical point, reveals a theoretical relation for the temperature dependence of K_D at near-critical conditions [59]

$$RT\ln K_D = 2A_{Kr}\cdot\frac{\left[\rho_{1,L}^* - \rho_{1,c}^*\right]}{\left(\rho_{1,c}^*\right)^2} \quad (12)$$

where L designates the liquid phase of water. In Eq. (12) the proper dimension of density is in mol cm^{-3}, with $\rho_{1,c}^* = 0.017874$ mol cm^{-3}. Analysis of available data shows that Equation (12) is valid not only close to the critical point, but is also reliable as much as 150 K below water's critical temperature, $T_c = 647.096$ K [58]. In order to obtain K_D values at from 298.15 to T_c, we applied a temperature function to Equation (12), similar to that proposed in Ref. [60]:

$$RT\ln K_D = 2A_{Kr}\frac{\left[\rho_{1,L}^* - \rho_{1,c}^*\right]}{\left(\rho_{1,c}^*\right)^2}\left(1 + a_1\tau + a_2\tau^{1.5} + a_3\tau^2 + a_4\tau^{2.5}\right) \quad (13)$$

where $\tau = 1 - T/T_c$. The parameters of Equation (13) are given in Table 3. For all solutes except Rn, values of A_{Kr} are taken from Ref. [31], and K_D values are from the recommendations of [58]. For Rn, for which no experimental high-temperature data exist, A_{Kr} has been estimated from the Gibbs energy of hydration at 298.15 K, as proposed in Ref. [32]. Estimation of K_D has been made as described in Ref. [61]: first, data for the enthalpy of hydration and

Table 2
Values of V_2^∞ simple fluids at 298.15 K, 0.1 MPa, see text.

Solute	V_2^∞(experimental) cm^3 mol^{-1}	Method[a]	V_2^∞(selected), cm^3 mol^{-1}	r_{vdW}, Å	r_{LJ}, Å	V_c, cm^3 mol^{-1}	α, Å^3	Estimated V_2^∞, cm^3 mol^{-1}	Accepted V_2^∞, cm^3 mol^{-1}
He	24.6 [b]	Vibr	**24.6 ± 3.0** [c]	1.40 [d]	1.28 [e]	37.5 [e,f]	0.208 [g]		
Ne				1.54 [d]	1.41 [e]	40.3 [e,f]	0.381 [g]	24.5 (Eq. (6))	24.6
								24.9 (Eq. (7))	
								24.5 (Eq. (9))	
								24.4 (Eq. (10))	
Ar	32.7 [b]	Vibr	**31.5 ± 1.7** [m]	1.88 [d]	1.77 [e]	74.57 [e]	1.664 [g]		
	31.0 [h]	MF							
	29.4 [i]	Pycn							
	32.6 [k]	Vibr							
	31.71 [l]	Dilat							
Kr	32.8 [k]	Vibr		2.02 [d]	1.83 [e]	91.20 [e]	2.498 [g]	35.4 (Eq. (6))	37.3
								38.4 (Eq. (7))	
								40.7 (Eq. (9))	
								34.8 (Eq. (10))	
Xe	42.7 [n]	Vibr		2.16 [d]	2.02 [e]	118.0 [e]	4.005 [g]	41.2 (Eq. (6))	45.0
								48.0 (Eq. (7))	
								47.6 (Eq. (9))	
								43.1 (Eq. (10))	
Rn				2.20 [o]		140.0 [e]	~4.8 [p]	45.9 (Eq. (6))	49.4
								52.4 (Eq. (7))	
								49.8 (Eq. (9))	
H_2	23.1 [b]	Vibr	**26.1 ± 1.3** [r]	1.36 [s,t]	1.41 [e]	51.5 [e,f]	0.787 [g]		
	26.7 [k]	Vibr							
	25.20 [l]	Dilat							
	26 [q]	Dilat							
N_2	33.1 [b]	Vibr	**34.7 ± 1.9** [m]	1.84 [v]	1.90 [e]	90.10 [e]	1.710 [g]		
	35.5 [i]	Pycn							
	34.3 [h]	MF							
	35.7 [k]	Vibr							
	40 [q,u]	Dilat							
O_2	32.1 [b]	Vibr	**31.4 ± 1.1** [m]	1.73 [v]	1.73 [e]	73.37 [e]	1.562 [g]		
	30.6 [i]	Pycn							
	31.1 [h]	MF							
	33.2 [k]	Vibr							
	30.38 [l]	Dilat							
	31 [q]	Dilat							
CO	37.3 [k]	Vibr	**36.7 ± 2.0** [c]	1.86 [v]	1.85 [e]	93.1 [e]	1.953 [g]		
	36 [q]	Dilat							
CH_4	32.0 [b,u]	Vibr	**37.0 ± 1.0** [m]	1.89 [v]	1.88 [e]	98.6 [e]	2.448 [g]		
	36.8 [w]	Vibr							
	34.5 [k,u]	Vibr							
	37.42 [l]	Dilat							
	36.3 [x]	Dilat							
	37 [q]	Dilat							

[a] Methods: Vibr – Vibrating tube; MF – Magnetic Float; Pycn – Pycnometer; Dilat – Dilatometer.
[b] [49].
[c] Our estimate of uncertainty.
[d] [54].
[e] [51].
[f] "Classical value", different for quantum fluids from measured values (57.3 for He, 41.70 for Ne, 64.2 for H_2).
[g] Computational Chemistry Comparison and Benchmark DataBase of NIST at http://cccbdb.nist.gov/exp2x.asp.
[h] [45].
[i] [46].
[k] [44.
[l] [43].
[m] the uncertainty for the confidence level of 0.95.
[n] [48], P = 33.41 MPa, i.e. the field of stability of a clathrate.
[o] [55].
[p] The online table of Schwerdtfeger P. at http://ctcp.massey.ac.nz/Tablepol2017.pdf.
[q] [41].
[r] as selected in Ref. [10].
[s] Calculated from the r_{vdW} for an atom and the bond distance l for diatomic molecule as explained in Ref. [54].
[t] r_{vdW} = 1.20 Å [54] and l = 0.741 Å
[u] not used as an outlier.
[v] calculated from the van der Waals volume of a molecule [54].
[w] [47], P is between 28 and 35 MPa.
[x] [42].

Table 3
Parameters of Equation (13) for the temperature dependence of K_D, including values of the Krichevskii parameter.

Solute	A_{Kr}, MPa	a_1	a_2	a_3	a_4
He	169[a]	−0.64158	2.6892	−4.7045	2.8472
Ne	186[a]	0.89014	−5.2142	7.3096	−3.1790
Ar	172[a]	2.1975	−11.567	18.343	−9.7146
Kr	169[a]	3.2541	−16.669	26.307	−13.870
Xe	150[a]	−0.77542	3.2312	−3.7738	0.68247
Rn	143[b]	−4.0737	12.064	−9.2242	0
H_2	170[a]	−2.1784	9.9059	−16.433	9.0854
N_2	178[a]	0.36979	−2.7266	4.7343	−2.8881
O_2	171[a]	0.23481	−1.9722	3.3344	−2.0638
CO	174[a]	2.5753	−13.013	20.252	−10.535
CH_4	164[a]	0.0	−0.49212	1.2971	−1.2985

[a] [31, including errata].
[b] [32].

the heat capacity of hydration of Rn in water at 298.15 K [62] allowed prediction of the Gibbs energies of hydration of Rn up to 473 K. These were converted into k_H values for Rn in the mole fraction scale. Then, vapor phase fugacity coefficients of Rn at infinite dilution in the aqueous vapor (V) phase, $\phi^{\infty}_{2,V}$, were calculated using B_{12} from Equation (4), leading to values of K_D found from $K_D = k_H/(P^*_{1,s}\phi^{\infty}_{2,V})$, where $P^*_{1,s}$ is the water saturation pressure. Finally, estimated values of A_{Kr} and K_D were fitted to Equation (13). The accuracy of our high-temperature results for Rn is not as good as for other gases, where K_D values are reliable to within a few percent for $T > 400$ K and are much more accurate for $T < 400$ K.

2.2.4. Estimation of A^{∞}_{12} values at densities of water between 500 and 900 kg m^{-3}

We have shown [9,29] that corresponding-states relations exist for the reduced A^{∞}_{12} function, $A^{\infty}_{12,\,red}$, defined as

$$A^{\infty}_{12,red} = \frac{A^{\infty}_{12}(T,\rho^*_1)}{A^{\infty}_{12}\left(T_r,\rho^*_{1,r}\right)} \tag{14}$$

where properties with the subscript r refer to 298.15 K and 0.1 MPa. Values of $A^{\infty}_{12,\,red}$ are quite similar within many classes of organic compounds (alcohols, amines, etc.) in water [9]. At specified conditions, the values of $A^{\infty}_{12,red}$ decrease from simple fluids to normal fluids to polar compounds to hydroxides [9,29]. Data-based values of $A^{\infty}_{12,\,red}$ are available up to 700 K. The extrapolation of $A^{\infty}_{12,\,red}$ to higher temperatures is based on the observation [9], following from the theory of mixtures of hard spheres [30], that the high-temperature limit of $A^{\infty}_{12,\,red}$ is equal to $A^{*}_{11,\,red}$, where $A^{*}_{11,red} = \frac{A^{*}_{11}(T,\rho^*_1)}{A^{*}_{11}(T_r,\rho^*_{1,r})}$ with the reduced bulk modulus, $A^{*}_{11} = \frac{V^{*}_{1}}{\kappa_T RT}$. Since $A^{*}_{11,\,red}$ is known with high precision up to very high T and P from an accurate water EoS [63], $A^{\infty}_{12,\,red}$ values are also known at $T > 1200$ K at moderate and high water densities. Note that while the IAPWS-95 EoS for water [63] was recommended only to 1273 K and 1 GPa, its authors stated that "IAPWS-95 can be extrapolated up to extremely high pressures and temperatures", giving us confidence that the properties up to 2000 K and 10 GPa are reliable. Combining experimental data at moderate temperatures and water densities with the known high-temperature limits, estimates of $A^{\infty}_{12,\,red}$ were made for several classes of solutes, including simple fluids, at water densities between 500 and 900 kg m^{-3} and temperatures from 600 K to 2000 K [9].

To extend the correlation for $A^{\infty}_{12,\,red}$ to ambient temperatures, high precision data for K_D can be used in the following way. Values of K_D can be obtained using Equation (1) for the liquid (L) and for the vapor (V) phases of water.

$$\ln K_D = \ln\frac{\phi^{\infty}_{2,L}}{\phi^{\infty}_{2,V}} = \int_{\rho^*_{1,V}}^{\rho^*_{1,L}} (A^{\infty}_{12} - 1)\,\frac{d\rho^*_1}{\rho^*_1} \tag{15}$$

Matching calculated and experimental K_D values constrains the variation of A^{∞}_{12} between the densities of coexisting vapor and liquid phases of water, which are not observable because they are in the metastable or unstable two-phase range.

This allows the use of two sources of information about $A^{\infty}_{12,\,red}$ of simple fluids at moderate water densities: 1) the precise experimental data on V^{∞}_2 for CH_4 [47], together with the somewhat less accurate V^{∞}_2 values for Ar [48] up to 700 K (the values at rounded water densities, obtained by interpolation of experimental data, are shown as stars in Fig. 3); and 2) values obtained by imposing agreement between experiment and values of K_D calculated from Equation (15) for Ar, chosen as the basis (values of $A^{\infty}_{12,\,red}$, estimated in this way, are shown as yellow circles in Fig. 3). The results from the various sources are shown in Fig. 3 with different symbols denoting the sources of the values. These data for $A^{\infty}_{12,\,red}$ from 298 to 2000 K at water densities of 500, 600, 700, 800 and 900 kg m^{-3} have been correlated as

$$A^{\infty}_{12,red} = a + bT + cT^2 \tag{16}$$

with the parameters a, b, and c given in Table 4.

2.3. Evaluation of the isothermal course of A^{∞}_{12} at various water densities

The above methods have been used to estimate A^{∞}_{12} as a function of T and ρ^*_1. A convenient representation for interpolation and smoothing of isothermal variations with water density is the function [9,15].

$$Y = (A^{\infty}_{12} - 1)/\rho^*_1 \tag{17}$$

which has a smaller range of variations compared to A^{∞}_{12}. At $\rho^*_1 = 0$ Equation (3) gives Y equal to $2B_{12}$, providing a high-precision intercept for Y. Estimated values of Y, as discussed above, are available at $\rho^*_1 \geq 500$ kg m^{-3}, and at near-critical temperatures and the critical density, through the Krichevskii parameter. Over the density range of 100–400 kg m^{-3}, we have no independent

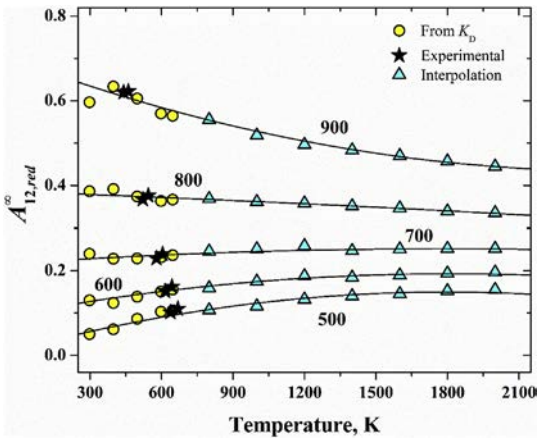

Fig. 3. Values $A^{\infty}_{12,red}$ for simple fluids in water from various sources of information. Curves are calculated with Equation (16) using parameters in Table 4. Numbers (500, …, 900) designate water densities in kg m^{-3}.

Table 4
Parameters of Equation (16) at different water densities.

ρ_1^*, kg m^{-3}	a	$10^4 b$, K^{-1}	$10^8 c$, K^{-2}
500	0.0147	1.512	−4.223
600	0.0987	10.42	−2.873
700	0.2179	3.796	−1.058
800	0.3849	−0.205	−0.249
900	0.6933	−2.074	4.145

estimates of A_{12}^{∞}, however, as experience shows, the contribution of this region to the integral for the fugacity coefficient, Eq. (1), is important. Therefore, over the density range of 100–400 kg m^{-3} we varied Y values to smoothly join the points between ρ_1^* equal to 0 and 500 kg m^{-3}, forming a convex function. The properly selected A_{12}^{∞} give at their integration, see Eq. (15), a good agreement with experimental values of K_D. Such a procedure was especially important for reliability when $T < 500$ K.

Fig. 4 shows Y for He and Xe in water at three temperatures: 298.15, 647.1 ($\approx T_c$), and 2000 K. The values at $\rho_1^* = 0$, have been calculated from B_{12} values from Eq. (4), with parameters from Table 1. The star at the critical temperature T_c and critical density has been calculated from Eq. (11) using A_{Kr} values in Table 3. The circles for $\rho_1^* = 500$–900 kg m^{-3} were calculated as described in Section 2.2.4 by using Eq. (16) to obtain $A_{12,red}^{\infty}$, and Eq. (14) to convert results to A_{12}^{∞} with V_2^{∞} at 298.15 K, 0.1 MPa from Table 2, while those for $\rho_1^* \geq 1000$ kg m^{-3} have been obtained from the hard-sphere relations of Section 2.2.2, Eq. (5), with V_2^{∞} at 298.15 K, 0.1 MPa from Table 2. Note that there are Y values along the 298.15 K isotherm at densities where two phases coexist, so these values are for metastable and unstable conditions. This is similar to the van der Waals loop for pure-component vapor-liquid equilibria from an EoS. The variation shown is required to reproduce experimental K_D values at 298.15 K. The lines in Fig. 4 are from the global formula described below.

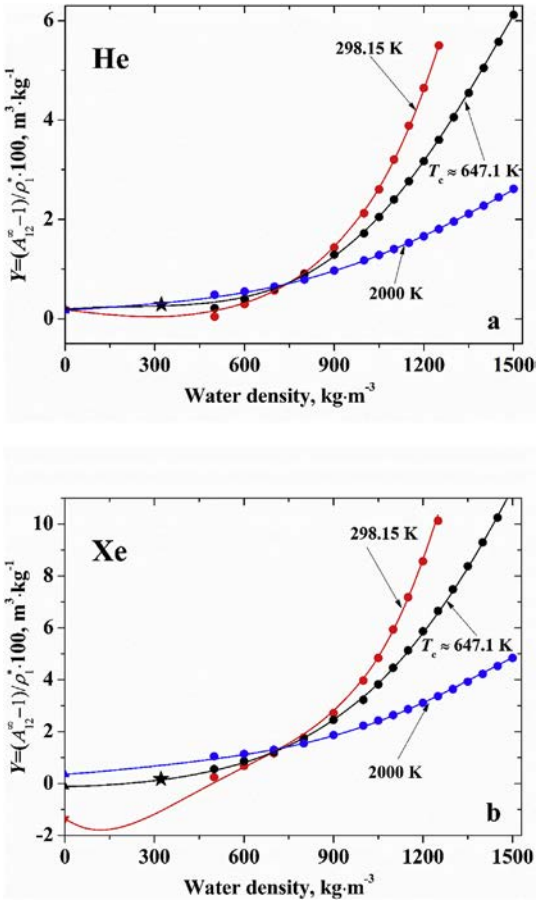

Fig. 4. Values of the auxiliary function Y of Equation (17) for He and Xe at infinite dilution in water at 298.15, 647.1, and 2000 K.

3. Results and discussion

3.1. Global fit of results

Tabulation of A_{12}^{∞} estimates was made for more 700 conditions for each solute for 13 temperatures between 298.15 and 623.15 K with a step of 25 K; at 633.15, 643.15, 647.10, 673.15 K; for nine temperatures between 700 and 1500 K with a step of 100 K; and at 1700 and 2000 K. The data were fitted with the function

$$A_{12}^{\infty} = 1 + \rho_1^* \left[a_o + a_1 \rho_1^* + a_2 (\rho_1^*)^2 + a_3 (\rho_1^*)^3 + a_4 (\rho_1^*)^4 + a_5 (\rho_1^*)^6 \right] \quad (18)$$

where

$$a_o = 2\Omega B_{12} \quad (19)$$

with $\Omega = \frac{10^{-3}}{M_w} \approx 55.508 \cdot 10^{-6}$ to convert B_{12} volume units of cm^3 mol^{-1} to m^3 kg^{-1}. The other temperature-dependent coefficients are

$$a_i = \sum_{n=1}^{7} a_{in} T_r^{-n} \quad (20)$$

where $T_r = T/T_c$ with $T_c = 647.096$ K [63]. For example, $a_1 = a_{11}T_r^{-1} + a_{12}T_r^{-2} + a_{13}T_r^{-3} + a_{14}T_r^{-4} + a_{15}T_r^{-5} + a_{16}T_r^{-6} + a_{17}T_r^{-7}$. An equation similar to Eq. (18) was used in Refs. [9,10], but without the a_4 term. It was found that addition of this term decreased the sum of squared errors by about 20–30%. Table 5 give the values of the a_{in}.

Evaluating Equation (1) gives infinite-dilution fugacity coefficients of solute (2) in solvent (1)

$$\ln \phi_2^{\infty} = \rho_1^* \left[a_o + \frac{a_1}{2}\rho_1^* + \frac{a_2}{3}(\rho_1^*)^2 + \frac{a_3}{4}(\rho_1^*)^3 + \frac{a_4}{5}(\rho_1^*)^4 + \frac{a_5}{7}(\rho_1^*)^6 \right] - \ln \frac{PV_1^*}{RT}, \quad (21)$$

where ρ_1^* is in kg m^{-3} and V_1^* is in cm^3 mol^{-1}.

3.2. Comparison with literature data at supercritical temperatures

3.2.1. Infinite-dilution fugacity coefficients

Fig. 5 (for $T = 750$ K) and Fig. 6 (for $T = 1500$ K) compare values of ϕ_2^{∞} from the presented method with those from three literature EoS: computer-simulation generated *PVTX* properties of binary water-gas systems (SUPERFLUID [11]), and [12], and a perturbation-theory EoS [13]. Figs. S1 and S2 of the Supplementary Materials show corresponding graphs for 1000 and 2000 K. Generally, results of all works are in reasonable agreement, although they are based on various computational approaches. Note that the EoS of [13] is not recommended for conditions of $T < 750$ K and $P < 50$ MPa; and SUPERFLUID EoS [11] for Ar and N_2 should not be used for $P < 500$ MPa. Our values at low supercritical temperatures are

Table 5
Parameters of Eq. (20) for different solutes.

$i\ n\rightarrow$ ↓	1	2	3	4	5	6	7
He							
1	$0.330171\cdot10^{-4}$	$-0.956234\cdot10^{-4}$	$1.66334\cdot10^{-4}$	$-1.64667\cdot10^{-4}$	$0.835003\cdot10^{-4}$	$-2.05151\cdot10^{-5}$	$1.96847\cdot10^{-6}$
2	$0.168282\cdot10^{-7}$	$-0.134021\cdot10^{-6}$	$0.162366\cdot10^{-6}$	$-0.0632820\cdot10^{-6}$	$0.111715\cdot10^{-7}$	$-0.0342337\cdot10^{-7}$	$0.0731267\cdot10^{-8}$
3	$0.296736\cdot10^{-10}$	$0.0354800\cdot10^{-9}$	$-0.115563\cdot10^{-9}$	$0.0630922\cdot10^{-9}$	$-0.00984355\cdot10^{-9}$	$0.00413077\cdot10^{-10}$	0
4	$-0.228315\cdot10^{-13}$	$0.0724047\cdot10^{-12}$	$-0.0251653\cdot10^{-12}$	0	$-0.0470755\cdot10^{-13}$	$0.283931\cdot10^{-14}$	$-0.485251\cdot10^{-15}$
5	$0.290321\cdot10^{-20}$	$-1.64964\cdot10^{-20}$	$1.08055\cdot10^{-20}$	$-1.41333\cdot10^{-21}$	0	0	0
Ne							
1	$0.272235\cdot10^{-4}$	$-0.990487\cdot10^{-4}$	$1.07231\cdot10^{-4}$	$-0.527256\cdot10^{-4}$	$0.215489\cdot10^{-4}$	$-0.977109\cdot10^{-5}$	$2.02335\cdot10^{-6}$
2	$0.146673\cdot10^{-7}$	$-0.0307540\cdot10^{-6}$	$0.374800\cdot10^{-6}$	$-0.573740\cdot10^{-6}$	$3.19327\cdot10^{-7}$	$-0.687621\cdot10^{-7}$	$0.364859\cdot10^{-8}$
3	$0.488631\cdot10^{-10}$	$-0.208907\cdot10^{-9}$	$-0.132675\cdot10^{-9}$	$0.414531\cdot10^{-9}$	$-0.232656\cdot10^{-9}$	$0.406685\cdot10^{-10}$	0
4	$-0.318303\cdot10^{-13}$	$0.207455\cdot10^{-12}$	$-0.126351\cdot10^{-12}$	0	$0.0192703\cdot10^{-13}$	$0.8040190\cdot10^{-14}$	$-2.40858\cdot10^{-15}$
5	$0.0843029\cdot10^{-20}$	$-1.53649\cdot10^{-20}$	$0.846021\cdot10^{-20}$	$-0.444989\cdot10^{-21}$	0	0	0
Ar							
1	$3.31120\cdot10^{-4}$	$-16.9690\cdot10^{-4}$	$34.2329\cdot10^{-4}$	$-34.5364\cdot10^{-4}$	$18.5501\cdot10^{-4}$	$-50.9746\cdot10^{-5}$	$56.4098\cdot10^{-6}$
2	$-6.38608\cdot10^{-7}$	$3.26991\cdot10^{-6}$	$-6.28720\cdot10^{-6}$	$5.93872\cdot10^{-6}$	$-29.5699\cdot10^{-7}$	$7.49049\cdot10^{-7}$	$-7.55633\cdot10^{-8}$
3	$5.22779\cdot10^{-10}$	$-2.26188\cdot10^{-9}$	$3.54594\cdot10^{-9}$	$-2.59097\cdot10^{-9}$	$0.902573\cdot10^{-9}$	$-1.24931\cdot10^{-10}$	0
4	$-1.57202\cdot10^{-13}$	$0.605600\cdot10^{-12}$	$-0.562860\cdot10^{-12}$	0	$2.46531\cdot10^{-13}$	$-12.3992\cdot10^{-14}$	$19.9139\cdot10^{-15}$
5	$1.10779\cdot10^{-20}$	$-4.96735\cdot10^{-20}$	$4.68195\cdot10^{-20}$	$-12.5029\cdot10^{-21}$	0	0	0
Kr							
1	$3.37502\cdot10^{-4}$	$-18.0856\cdot10^{-4}$	$37.8160\cdot10^{-4}$	$-38.9855\cdot10^{-4}$	$21.0871\cdot10^{-4}$	$-57.5198\cdot10^{-5}$	$62.4522\cdot10^{-6}$
2	$-5.89268\cdot10^{-7}$	$3.45089\cdot10^{-6}$	$-7.26941\cdot10^{-6}$	$7.27048\cdot10^{-6}$	$-37.0316\cdot10^{-7}$	$9.23612\cdot10^{-7}$	$-8.83522\cdot10^{-8}$
3	$3.15911\cdot10^{-10}$	$-1.92919\cdot10^{-9}$	$3.93134\cdot10^{-9}$	$-3.52677\cdot10^{-9}$	$1.43707\cdot10^{-9}$	$-2.18517\cdot10^{-10}$	0
4	$0.227397\cdot10^{-13}$	$0.136816\cdot10^{-12}$	$-0.255015\cdot10^{-12}$	0	$2.35063\cdot10^{-13}$	$-15.1326\cdot10^{-14}$	$28.2990\cdot10^{-15}$
5	$-1.48330\cdot10^{-20}$	$2.42315\cdot10^{-20}$	$-1.61166\cdot10^{-20}$	$4.71965\cdot10^{-21}$	0	0	0
Xe							
1	$2.46371\cdot10^{-4}$	$-14.2013\cdot10^{-4}$	$32.3087\cdot10^{-4}$	$-35.7220\cdot10^{-4}$	$20.1886\cdot10^{-4}$	$-56.5366\cdot10^{-5}$	$62.4672\cdot10^{-6}$
2	$-2.59311\cdot10^{-7}$	$2.31057\cdot10^{-6}$	$-6.14630\cdot10^{-6}$	$7.10728\cdot10^{-6}$	$-38.8621\cdot10^{-7}$	$9.95998\cdot10^{-7}$	$-9.55320\cdot10^{-8}$
3	$-0.659378\cdot10^{-10}$	$-0.662369\cdot10^{-9}$	$2.91966\cdot10^{-9}$	$-3.67398\cdot10^{-9}$	$1.73832\cdot10^{-9}$	$-2.81519\cdot10^{-10}$	0
4	$1.98125\cdot10^{-13}$	$-0.453872\cdot10^{-12}$	$0.241266\cdot10^{-12}$	0	$1.75538\cdot10^{-13}$	$-15.7832\cdot10^{-14}$	$33.5822\cdot10^{-15}$
5	$-2.96836\cdot10^{-20}$	$8.00940\cdot10^{-20}$	$-7.34314\cdot10^{-20}$	$19.0536\cdot10^{-21}$	0	0	0
Rn							
1	$2.29992\cdot10^{-4}$	$-16.5568\cdot10^{-4}$	$44.6590\cdot10^{-4}$	$-57.1003\cdot10^{-4}$	$37.1623\cdot10^{-4}$	$-119.633\cdot10^{-5}$	$151.402\cdot10^{-6}$
2	$-5.73390\cdot10^{-7}$	$4.51594\cdot10^{-6}$	$-11.2419\cdot10^{-6}$	$13.0822\cdot10^{-6}$	$-77.5109\cdot10^{-7}$	$22.7877\cdot10^{-7}$	$-26.3489\cdot10^{-8}$
3	$5.91825\cdot10^{-10}$	$-3.95159\cdot10^{-9}$	$7.84421\cdot10^{-9}$	$-6.92661\cdot10^{-9}$	$2.80369\cdot10^{-9}$	$-4.30147\cdot10^{-10}$	0
4	$-1.57576\cdot10^{-13}$	$1.08196\cdot10^{-12}$	$-1.30155\cdot10^{-12}$	0	$8.63588\cdot10^{-13}$	$-51.0940\cdot10^{-14}$	$91.6656\cdot10^{-15}$
5	$-0.0431787\cdot10^{-20}$	$-4.66333\cdot10^{-20}$	$5.66059\cdot10^{-20}$	$-17.4462\cdot10^{-21}$	0	0	0
H_2							
1	$1.02969\cdot10^{-4}$	$-3.77391\cdot10^{-4}$	$5.15786\cdot10^{-4}$	$-3.10456\cdot10^{-4}$	$0.670948\cdot10^{-4}$	$0.581482\cdot10^{-5}$	$-3.01150\cdot10^{-6}$
2	$-1.51880\cdot10^{-7}$	$0.454209\cdot10^{-6}$	$-0.320341\cdot10^{-6}$	$-0.126678\cdot10^{-6}$	$2.59977\cdot10^{-7}$	$-1.164377\cdot10^{-7}$	$1.74266\cdot10^{-8}$
3	$2.25633\cdot10^{-10}$	$-0.614891\cdot10^{-9}$	$0.474883\cdot10^{-9}$	$-0.144575\cdot10^{-9}$	$0.0214011\cdot10^{-9}$	$-0.0229158\cdot10^{-10}$	0
4	$-1.06420\cdot10^{-13}$	$0.304710\cdot10^{-12}$	$-0.155026\cdot10^{-12}$	0	$-0.0232358\cdot10^{-13}$	$0.795336\cdot10^{-14}$	$-1.67248\cdot10^{-15}$
5	$1.18910\cdot10^{-20}$	$-4.03882\cdot10^{-20}$	$2.50264\cdot10^{-20}$	$-3.25879\cdot10^{-21}$	0	0	0
N_2							
1	$1.71614\cdot10^{-4}$	$-7.87088\cdot10^{-4}$	$14.4505\cdot10^{-4}$	$-13.1668\cdot10^{-4}$	$6.31582\cdot10^{-4}$	$-15.4929\cdot10^{-5}$	$15.4923\cdot10^{-6}$
2	$-2.11747\cdot10^{-7}$	$1.05405\cdot10^{-6}$	$-1.87483\cdot10^{-6}$	$1.55157\cdot10^{-6}$	$-6.40910\cdot10^{-7}$	$1.32852\cdot10^{-7}$	$-1.15412\cdot10^{-8}$
3	$1.63879\cdot10^{-10}$	$-0.636905\cdot10^{-9}$	$0.858253\cdot10^{-9}$	$-0.486214\cdot10^{-9}$	$0.100180\cdot10^{-9}$	$-0.0328645\cdot10^{-10}$	0
4	$-0.439095\cdot10^{-13}$	$0.204020\cdot10^{-12}$	$-0.162376\cdot10^{-12}$	0	$0.427314\cdot10^{-13}$	$-1.24034\cdot10^{-14}$	$0.473523\cdot10^{-15}$
5	$0.270801\cdot10^{-20}$	$-2.12050\cdot10^{-20}$	$1.73572\cdot10^{-20}$	$-3.34712\cdot10^{-21}$	0	0	0
O_2							
1	$1.14609\cdot10^{-4}$	$-4.78505\cdot10^{-4}$	$8.15298\cdot10^{-4}$	$-6.79959\cdot10^{-4}$	$2.83409\cdot10^{-4}$	$-5.55452\cdot10^{-5}$	$3.85476\cdot10^{-6}$
2	$-0.995565\cdot10^{-7}$	$0.418916\cdot10^{-6}$	$-0.665720\cdot10^{-6}$	$0.465682\cdot10^{-6}$	$-1.17181\cdot10^{-7}$	$-0.0324792\cdot10^{-7}$	$0.364776\cdot10^{-8}$
3	$0.742646\cdot10^{-10}$	$-0.168799\cdot10^{-9}$	$0.132150\cdot10^{-9}$	$-0.0453310\cdot10^{-9}$	$-0.00489050\cdot10^{-9}$	$0.0424158\cdot10^{-10}$	0
4	$-0.160987\cdot10^{-13}$	$0.0654708\cdot10^{-12}$	$-0.0108608\cdot10^{-12}$	0	$-0.210736\cdot10^{-13}$	$1.41196\cdot10^{-14}$	$-2.73644\cdot10^{-15}$
5	$0.0811105\cdot10^{-20}$	$-1.09479\cdot10^{-20}$	$0.470839\cdot10^{-20}$	$0.960803\cdot10^{-21}$	0	0	0
CO							
1	$2.98880\cdot10^{-4}$	$-15.5113\cdot10^{-4}$	$31.4220\cdot10^{-4}$	$-31.4446\cdot10^{-4}$	$16.4808\cdot10^{-4}$	$-43.4599\cdot10^{-5}$	$45.4478\cdot10^{-6}$
2	$-4.58140\cdot10^{-7}$	$2.51278\cdot10^{-6}$	$-4.97136\cdot10^{-6}$	$4.69613\cdot10^{-6}$	$-22.6036\cdot10^{-7}$	$5.31538\cdot10^{-7}$	$-4.72948\cdot10^{-8}$
3	$3.07899\cdot10^{-10}$	$-1.43490\cdot10^{-9}$	$2.38664\cdot10^{-9}$	$-1.83690\cdot10^{-9}$	$0.666573\cdot10^{-9}$	$-0.939165\cdot10^{-10}$	0
4	$-0.654523\cdot10^{-13}$	$0.303023\cdot10^{-12}$	$-0.274778\cdot10^{-12}$	0	$1.08504\cdot10^{-13}$	$-5.24611\cdot10^{-14}$	$8.04952\cdot10^{-15}$
5	$0.388032\cdot10^{-20}$	$-2.63707\cdot10^{-20}$	$2.35466\cdot10^{-20}$	$-4.84078\cdot10^{-21}$	0	0	0

Table 5 (*continued*)

$i\ n\rightarrow$ ↓	1	2	3	4	5	6	7
CH_4							
1	$2.97057\cdot10^{-4}$	$-16.1247\cdot10^{-4}$	$34.4063\cdot10^{-4}$	$-36.0221\cdot10^{-4}$	$19.5874\cdot10^{-4}$	$-53.2147\cdot10^{-5}$	$57.0850\cdot10^{-6}$
2	$-4.49849\cdot10^{-7}$	$2.93254\cdot10^{-6}$	$-6.71023\cdot10^{-6}$	$7.07104\cdot10^{-6}$	$-36.8944\cdot10^{-7}$	$9.22213\cdot10^{-7}$	$-8.66110\cdot10^{-8}$
3	$1.61007\cdot10^{-10}$	$-1.37627\cdot10^{-9}$	$3.44496\cdot10^{-9}$	$-3.48885\cdot10^{-9}$	$1.51742\cdot10^{-9}$	$-2.38812\cdot10^{-10}$	0
4	$0.766418\cdot10^{-13}$	$-0.0700448\cdot10^{-12}$	$-0.0767257\cdot10^{-12}$	0	$1.97840\cdot10^{-13}$	$-14.2101\cdot10^{-14}$	$28.0351\cdot10^{-15}$
5	$-1.50262\cdot10^{-20}$	$3.06667\cdot10^{-20}$	$-2.51644\cdot10^{-20}$	$6.99891\cdot10^{-21}$	0	0	0

closest to those of [13], while at the highest temperature, 2000 K, our results usually are higher than all literature EoS. This would lead to lower concentrations than from other models at the same conditions. Generally, high-temperature thermodynamic properties of simple fluids at high dilution in water appears to be reasonably well constrained by consistent results of several studies, including the current one: at densities above 1000 K the agreement of various EoS is usually within 1 $\log_{10}$ unit, which likely reflects the uncertainty of high-density predictions. In the absence of precise experimental results at supercritical temperatures, a more definite conclusion is not warranted.

3.3. Comparison with literature data at subcritical temperatures

Data on the properties of dilute solutions of simple fluids in water at subcritical temperatures are known with high precision, especially at temperatures below 373 K. For example, see recommendations on values of k_H and K_D by Fernández-Prini et al. [58]. This section compares our results with these recommendations.

3.3.1. Comparisons of K_D and introduction of reference K_D values

As discussed in Section 2.2.4, Equation (15) allows the calculation of K_D from the "volumetric" information

$$\ln K_D = \ln \phi^{\infty}_{2,L} - \ln \phi^{\infty}_{2,V} \tag{22}$$

where L and V designate the coexisting liquid and vapor phases of water. Fig. 7 shows comparisons of the recommended values of $\ln K_D$ [58] with those calculated from Equation (22). In all cases, the difference is less than 0.11 ln units (less than 0.05 $\log_{10}$ units) or 11%. Unfortunately, this accuracy in K_D is not within the experimental uncertainty of 1% at temperatures below 373 K.

It is expected that the principal error in the present model is in the calculation of $\phi^{\infty}_{2,L}$. To improve upon our accuracy, fugacity coefficients of solutes for liquid, $\phi^{\infty}_{2,L}$, have been evaluated from

$$\ln \phi^{\infty}_{2,L} = \ln K_D(recom) + \ln \phi^{\infty}_{2,V} \tag{23}$$

with $\ln K_D(recom)$ calculated from Equation (13). The corrected values of $\phi^{\infty}_{2,L}$ are given in the Excel file "Supplementary Materials".

3.3.2. Comparison of Henry's constants

Henry's constant, k_H, is defined in Ref. [58] as

$$k_H = \lim_{x_2 \to 0} (f_2/x_2) \tag{24}$$

where f_2 and x_2 are the fugacity and mole fraction of a solute. The fugacity of a solute is given by $f_2 = P\phi_2 x_2$ [50]. Applying this definition to the vapor-liquid envelope of water, the relation between k_H and K_D is [26,59]:

$$k_H = K_D \phi^{\infty}_{2,V} P^*_{1,s} \tag{25}$$

with $P^*_{1,s}$ the water saturation pressure. Using K_D values computed with Equation (13) in Equation (25), Henry's constants have been calculated for the solutes under consideration and compared with the recommendations of [58]. The results are shown in Fig. 8.

For Xe, N_2, and O_2 over the whole temperature range from 298.15 to 647.1 K (T_c) the agreement of recommended k_H values with those from Equation (25) is very good, within 0.08 ln units (<0.04 $\log_{10}$ units); for Ne, Ar, and CH_4 the agreement is satisfactory – within 0.18 ln units (<0.08 $\log_{10}$ units). However, for He, Kr, and H_2 the deviations increase significantly as T increases above 600 K. At 647.1 K (T_c) the differences are 1.3, 0.45, and 0.68 ln units, respectively (~0.6, 0.2 and 0.3 $\log_{10}$ units). For CO, the disagreement begins at lower temperatures, growing from ~0.2 ln units (~0.09 $\log_{10}$ units) at 500 K to more than 0.4 ln units (~0.18 $\log_{10}$ units) for $T > 550$ K. The greatest deviations are generally at temperatures above those of the measurements.

The differences arise from using the present calculated values of $\phi^{\infty}_{2,V}$ and those estimated in Ref. [58] that employed the Peng-Robinson EOS. To assess which result should be accepted, values of $\phi^{\infty}_{2,V}$ have been calculated using B_{12} with Eq. (26) that should be sufficiently accurate up to approximately 1/2 the water critical density:

$$\ln \phi^{\infty}_{2,V} \approx \frac{2}{V^*_1} B_{12} - \ln \frac{PV^*_1}{RT} \tag{26}$$

The density of saturated water at $T \sim 633$ K is $\rho^*_1 \approx 144\ \mathrm{kg\ m^{-3}}$ or ~45% of the critical water density. Fig. 9 compares $\phi^{\infty}_{2,V}$ values from: 1) k_H and K_D data of [58]; 2) results of this work; 3) Equation (26) for He and CO. The Supplementary Material shows the results for all solutes where a comparison is possible.

Because the correct lower density formulation with B_{12} is incorporated in the present approach, the overall results of this work are very close to those from predictions of Equation (26). For He and CO, values of $\phi^{\infty}_{2,V}$ employed in Ref. [58] at temperatures above 450–500 K are systematically lower those evaluated from the truncated virial EoS. This suggests that the recommended values for k_H should be revised at least for He and CO.

Japas and Levelt Sengers [59] have derived a linear relationship for the asymptotic variation of k_H near the solvent's critical point,

$$RT \ln \frac{k_H}{f^*_1} = h_0 + A_{Kr} \frac{\left(\rho^*_{1,L} - \rho^*_{1,c}\right)}{\left(\rho^*_{1,c}\right)^2} \tag{27}$$

where f^*_1 is the pure water fugacity, which can be calculated using an EoS for H_2O [63]. The present work suggests that the last term in Equation (27) should be appended by an expanded form, similar to that of Equation (13). This leads to a correlation that accurately reproduces k_H from 298.15 to 647.1 K ($\tau = 1 - T/T_c$):

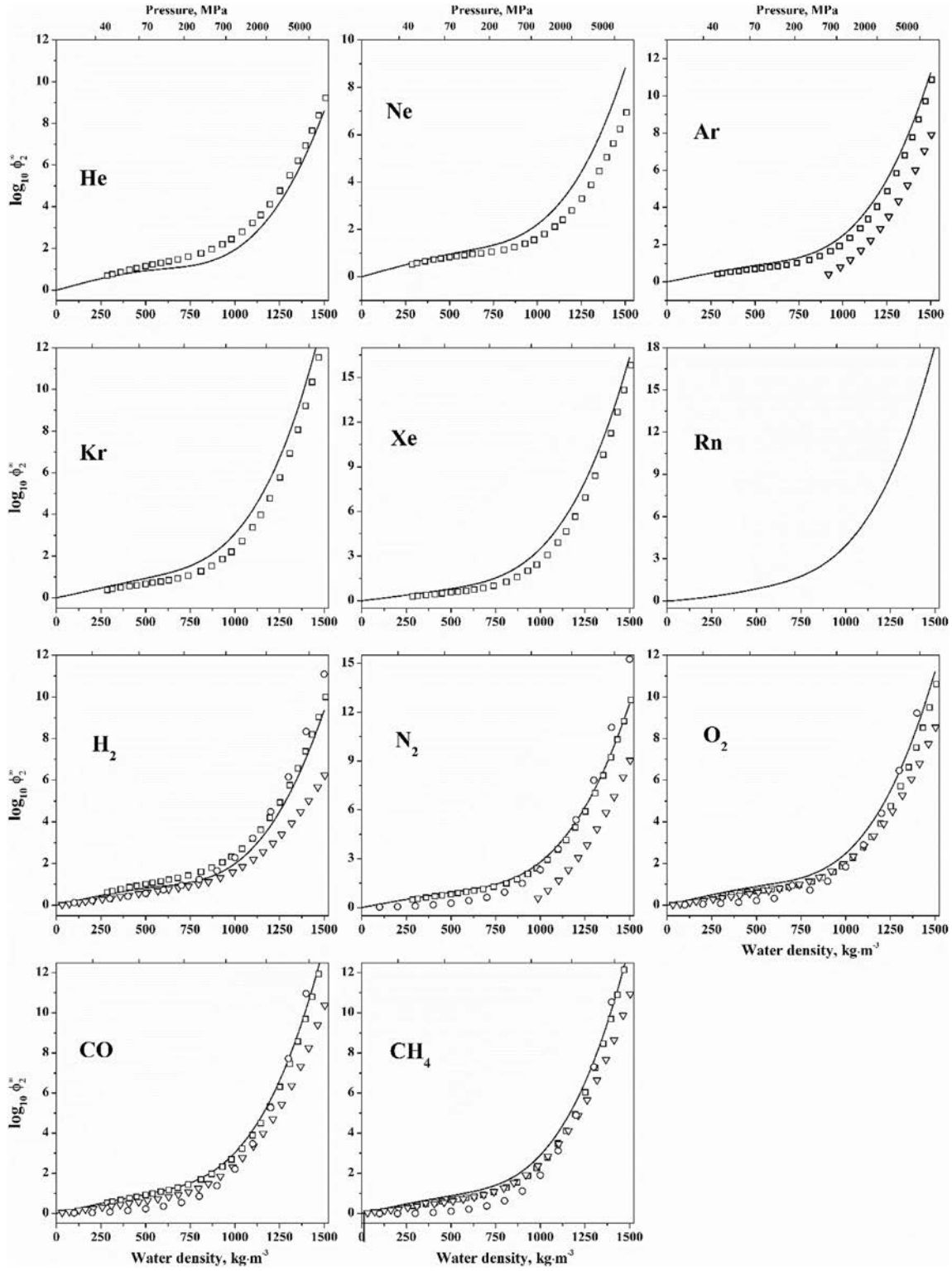

Fig. 5. Comparison of predictions of this work (lines) at 750 K with results of literature EoS, given by symbols: triangles – [11], circles ([12], coded by Ref. [14]), squares – [13].

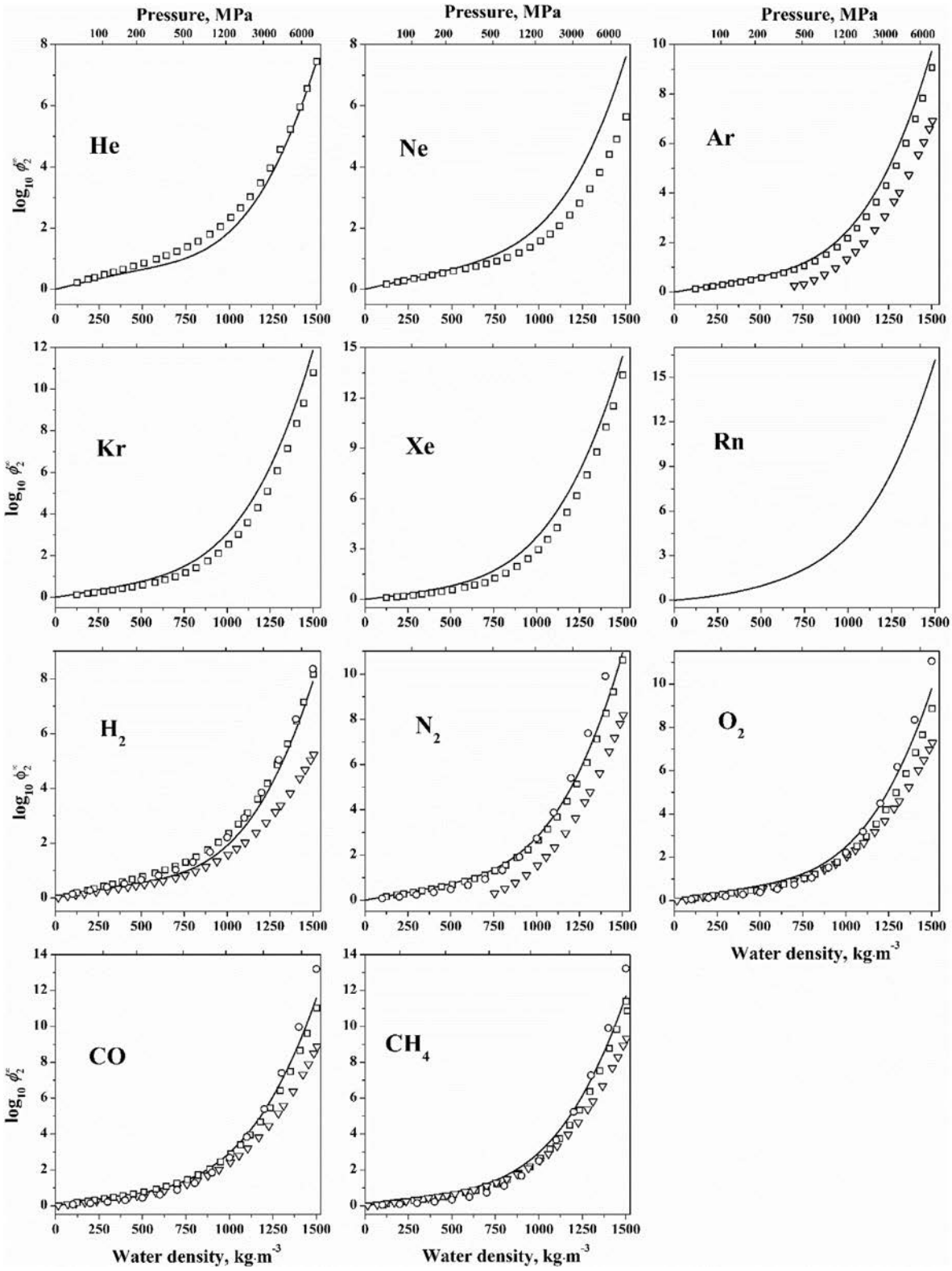

Fig. 6. Comparison of predictions of this work (lines) at 1500 K with results of literature EoS, given by symbols: triangles – [11], circles ([12], coded by Ref. [14]), squares – [13].

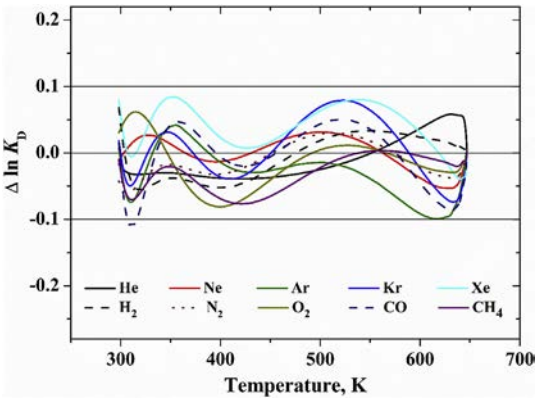

Fig. 7. The difference between recommended values of lnK_D [58] and those calculated with Equation (22).

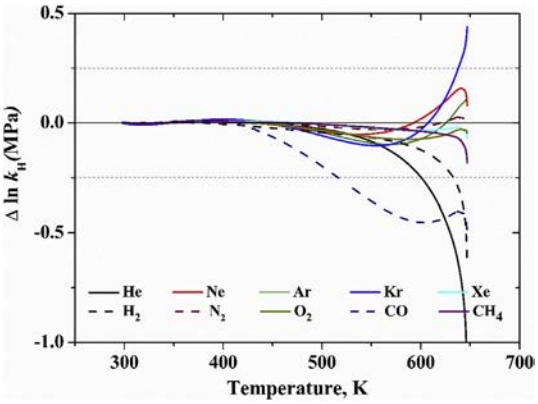

Fig. 8. Differences between recommended values of lnk_H [58] and those calculated with Equation (25).

$$RT\ln\frac{k_H}{f_1^*}=h_0+A_{Kr}\frac{\left(\rho_{1,L}^*-\rho_{1,c}^*\right)}{\left(\rho_{1,c}^*\right)^2}\left(1+h_1\tau^{1.25}+h_2\tau^{1.5}+h_3\tau^{1.75}+h_4\tau^2\right). \tag{28}$$

where the parameters $h_0 - h_4$ are given in Table 6. This relation should not be used at temperatures outside of 298–647.1 K.

3.3.3. Calculation of ϕ_2^∞ at high pressures (water densities) below T_c

Values of ϕ_2^∞ along subcritical isotherms ($T < 647.1$ K) for compressed liquid water (for $P > P_{1,s}^*$, the water saturation pressure) can be obtained from

$$\ln\phi_2^\infty=\ln\phi_{2,L}^\infty+\rho_1^*\left[a_o+\frac{a_1}{2}\rho_1^*+\frac{a_2}{3}(\rho_1^*)^2+\frac{a_3}{4}(\rho_1^*)^3+\frac{a_4}{5}(\rho_1^*)^4+\frac{a_5}{7}(\rho_1^*)^6\right]-\rho_{1,s}^*\left[a_o+\frac{a_1}{2}\rho_{1,s}^*+\frac{a_2}{3}\left(\rho_{1,s}^*\right)^2+\frac{a_3}{4}\left(\rho_{1,s}^*\right)^3+\frac{a_4}{5}\left(\rho_{1,s}^*\right)^4+\frac{a_5}{7}\left(\rho_{1,s}^*\right)^6\right]-\ln\frac{P\,\rho_{1,s}^*}{P_{1,s}^*\,\rho_1^*}, \tag{29}$$

where $\rho_{1,s}^*$ is the density of liquid water at $P_{1,s}^*$ and ln $\phi_{2,L}^\infty$ is defined in Equation (23). Fig. 7 shows that the correction is small, always < 0.11 ln unit.

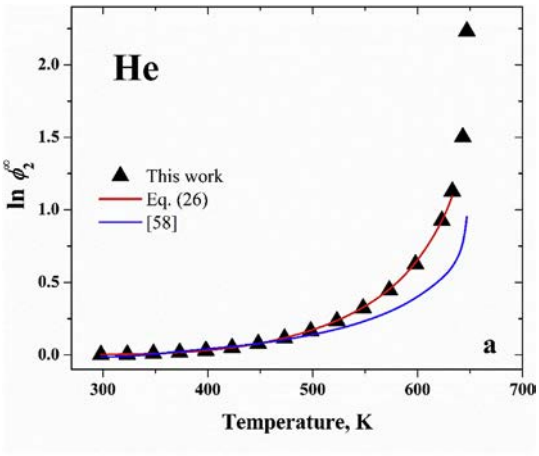

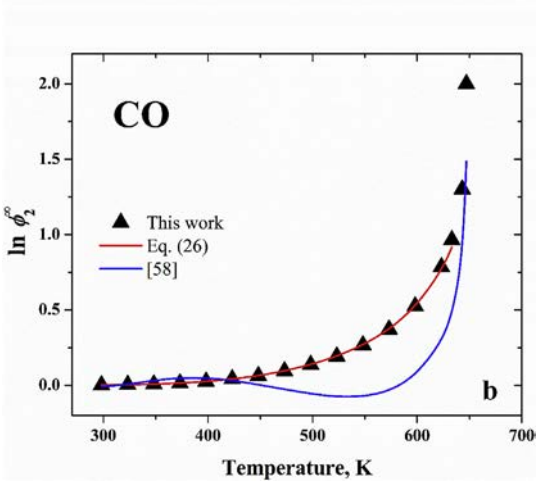

Fig. 9. The values of the fugacity coefficients evaluated in this work, calculated with Equation (26) and determined from k_H and K_D data of [58] for (a) He and (b) CO.

Table 6
Values of parameters $h_0 - h_4$ of Equation (28) for calculating Henry's constants, k_H, of solutes in water for T from 298.15 to 647.1 K.

Solute	h_0, J mol^{-1}	h_1	h_2	h_3	h_4
He	14101.4	−16.7925	64.5104	−79.1439	31.8977
Ne	14003.0	39.5335	−138.405	163.732	−65.1344
Ar	13082.5	49.6717	−181.137	225.384	−95.0142
Kr	12448.0	70.1943	−255.179	314.861	−131.292
Xe	10168.7	40.0254	−136.713	168.492	−73.2324
Rn	8611.8	28.5425	−128.408	198.412	−101.063
H_2	13008.3	2.97582	−3.69394	0	0.871058
N_2	13270.4	27.2763	−95.0488	117.070	−50.1020
O_2	13158.3	26.5351	−95.6743	120.939	−52.6848
CO	13017.7	72.6866	−266.528	331.484	−139.000
CH_4	12327.5	20.3832	−68.5418	84.8780	−37.5232

4. Summary

Equations with parameters have been given for the thermodynamic properties of He, Ne, Ar, Kr, Xe, Rn, H_2, N_2, O_2, CO, and CH_4 at infinite dilution in water from 298 to 2000 K and water densities from 0 to 1500 kg m^{-3}. Eq. (18) gives the correlation for A_{12}^∞. Eq. (21) gives the solute infinite-dilution fugacity coefficient, lnϕ_2^∞. This equation can be used directly at the critical isotherm and above, though small corrections are recommended at subcritical temperatures, in order to achieve the agreement with the vapor-liquid distribution coefficients, K_D of Eq. (13). In particular, we

recommend using the small correction of Eq. (23) for the values of the $\phi^{\infty}_{2,L}$, the fugacity coefficient of an infinitely diluted solute in a liquid phase of water at saturation, calculated with Eq. (21). The values of Henry's constants, k_H, consistent with K_D and fugacity coefficients for solutes in the vapor phase of water ($\phi^{\infty}_{2,V}$, calculated with Eq. (21)) are given by Eq. (28) over temperatures from 298.15 to 647.1 K. Calculated A^{∞}_{12} and ϕ^{∞}_{2} for all solutes at various T and P are tabulated in the Supplementary Material in an Excel file.

Examples are shown for aqueous methane. Fig. 10a shows A^{∞}_{12} for dissolved methane as a function of water density at various temperatures. Fig. 10b shows $\log_{10}\phi^{\infty}_{2}$ at the same conditions. The partial Gibbs energy may be defined as

$$G_2 = RT \ln \frac{P\phi^{\infty}_{2}}{P^{\circ}} \tag{30}$$

where $P^{\circ} = 0.1$ MPa for pressures given in MPa. Fig. 10c shows G_2 as a function of water density at various temperatures for dissolved methane. Note that values of $\log_{10}\phi^{\infty}_{2}$ pass through minima at subcritical temperatures, though these are not seen in G_2.

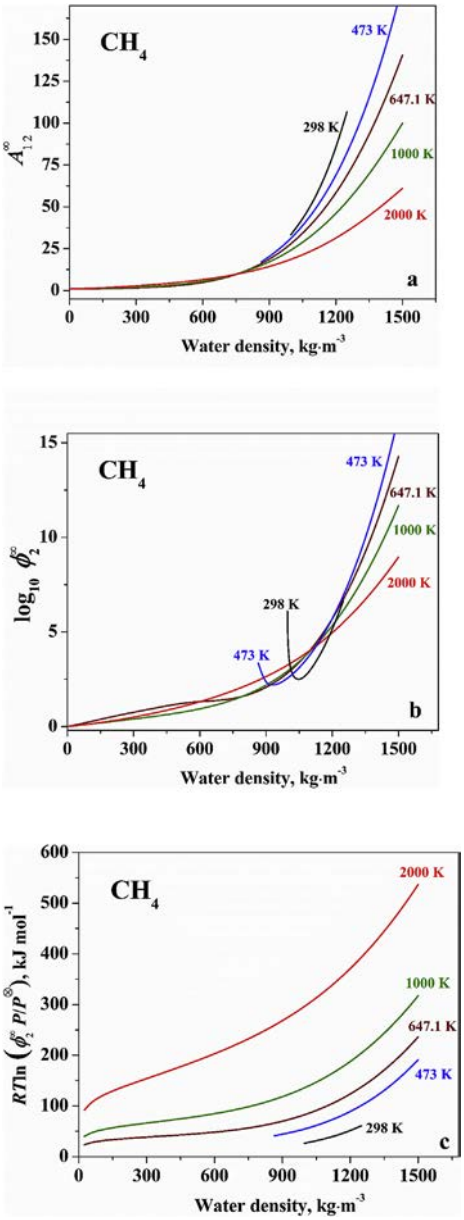

Fig. 10. Values of A^{∞}_{12} (a), $\log_{10}\phi^{\infty}_{2}$ (b), and G_2 (c) of infinitely dilute CH_4 in water over wide T and ρ^{*}_{1} ranges.

5. Conclusions

Equations have been developed for several thermodynamic properties of simple fluid solutes at infinite dilution in water from 298 to 2000 K and water densities from 0 to 1500 kg m^{-3}. For this entire range of conditions, the method based on Fluctuation Solution Theory requires only very limited and well-known property values: the partial molar volume at infinite dilution, V^{∞}_{2}, of the solute at 298.15 K; the second cross virial coefficient of the solute with water, B_{12}, and the solute's Krichevskii parameter, A_{Kr}.

Fugacity coefficients, ϕ^{∞}_{2}, at supercritical temperatures agree reasonably with results of prior studies, suggesting that high-temperature thermodynamic properties of simple fluids at high dilution in water can now be considered known within restricted uncertainties. Small corrections were required to achieve agreement with the recommended [58] constants of distribution of solutes between the vapor and liquid phases of water, k_D. Comparisons of calculated Henry's constants with recommendations [58] suggest revision of results for some solutes when $T > 550$ K.

Acknowledgements

This research was partially supported by Russian Foundation for Basic Research (grant 18-05-00462a).

Appendix A. Supplementary data

Supplementary data to this article can be found online at https://doi.org/10.1016/j.fluid.2019.06.012.

References

[1] H.C. Helgeson, D.H. Kirkham, G.C. Flowers, Theoretical prediction of the thermodynamic behavior of aqueous electrolytes at high pressures and temperatures. IV. Calculation of activity coefficients, osmotic coefficients, and apparent molal and standard and relative partial molal properties to 5 kb and 600°C, Am. J. Sci. 281 (10) (1981) 1241–1516. https://doi.org/10.2475/ajs.281.10.1249.

[2] J.C. Tanger, H.C. Helgeson, Calculation of the thermodynamic and transport properties of aqueous species at high pressures and temperatures: revised equations of state for the standard partial molal properties of ions and electrolytes, Am. J. Sci. 288 (1) (1988) 19–98. https://doi.org/10.2475/ajs.288.1.19.

[3] E.L. Shock, H.C. Helgeson, D.A. Sverjensky, Calculation of the thermodynamic and transport properties of aqueous species at high pressures and temperatures: standard partial molal properties of inorganic neutral species, Geochem. Cosmochim. Acta 53 (9) (1989) 2157–2184. https://doi.org/10.1016/0016-7037(89)90341-4.

[4] D.A. Sverjensky, B. Harrison, D. Azzolini, Water in the deep Earth: the dielectric constant and the solubilities of quartz and corundum to 60 kb and 1200°C, Geochem. Cosmochim. Acta 129 (2014) 125–145. https://doi.org/10.1016/j.gca.2013.12.019.

[5] A.V. Plyasunov, Estimation of the Henry constant of apolar gases at temperatures above the critical temperature of water, Dokl. Akad. Nauk 321 (5) (1991) 1071–1074 (in Russian).

[6] C.-L. Lin, R.H. Wood, Prediction of the free energy of dilute aqueous methane, ethane, and propane at temperatures from 600 to 1200° C and densities from 0 to 1 g cm-3 using molecular dynamics simulations, J. Phys. Chem. 100 (4) (1996) 16399–16409. https://doi.org/10.1021/jp961169v.

[7] J.P. O'Connell, A.V. Sharygin, R.H. Wood, Infinite dilution partial molar volumes of aqueous solutes over wide ranges of conditions, Ind. Eng. Chem. Res. 35 (8) (1996) 2808–2812. https://doi.org/10.1021/ie950729u.

[8] N.N. Akinfiev, L.W. Diamond, Thermodynamic description of aqueous nonelectrolytes at infinite dilution over a wide range of state parameters, Geochem. Cosmochim. Acta 67 (4) (2003) 613–627. https://doi.org/10.1016/S0016-7037(02)01141-9.

[9] A.V. Plyasunov, Correlation and prediction of thermodynamic properties of nonelectrolytes at infinite dilution in water over very wide temperature and pressure ranges (2000 K and 10 GPa), Geochem. Cosmochim. Acta 168 (2015) 236–260. https://doi.org/10.1016/j.gca.2015.07.012.

[10] A.V. Plyasunov, E.F. Bazarkina, Thermodynamic properties of dilute hydrogen in supercritical water, Fluid Phase Equilib. 470 (2018) 140–148. https://doi.

org/10.1016/j.fluid.2017.11.004.
[11] A.B. Belonoshko, P. Shi, S.K. Saxena, SUPERFLUID: a FORTRAN-77 program for calculation of Gibbs free energy and volume of C-H-O-N-S-Ar mixtures, Comput. Geosci. 18 (9) (1992) 1267–1269. https://doi.org/10.1016/0098-3004(92)90044-R.
[12] Z. Duan, N. Møller, J.H. Weare, A general equation of state for supercritical fluid mixtures and molecular dynamics simulation of mixture PVTX properties, Geochem. Cosmochim. Acta 60 (7) (1996) 1209–1216. https://doi.org/10.1016/0016-7037(96)00004-X.
[13] S.S. Churakov, M. Gottschalk, Perturbation theory based equation of state for polar molecular fluids: II. Fluid mixtures, Geochem. Cosmochim. Acta 67 (13) (2003) 2415–2425. https://doi.org/10.1016/S0016-7037(02)01348-0.
[14] R.J. Bakker, Package FLUIDS 1. Computer programs for analysis of fluid inclusion data and for modelling bulk fluid properties, Chem. Geol. 194 (1) (2003) 3–23. https://doi.org/10.1016/S0009-2541(02)00268-1.
[15] A.V. Plyasunov, Theory-based constraints on variations of infinite dilution partial molar volumes of aqueous solutes at various temperatures and water densities, Fluid Phase Equilib. 375 (2014) 11–17. https://doi.org/10.1016/j.fluid.2014.04.024.
[16] J.M.H. Levelt Sengers, How Fluids Unmix. Discoveries by the School of Van der Waals and Kamerlingh Onnes. Edita, KNAW, Amsterdam, 2002.
[17] J. Sedlbauer, J.P. O'Connell, R.H. Wood, A new equation of state for correlation and prediction of standard molal thermodynamic properties of aqueous species at high temperatures and pressures, Chem. Geol. 163 (1) (2000) 43–63. https://doi.org/10.1016/S0009-2541(99)00133-3.
[18] A.V. Plyasunov, J.P. O'Connell, R.H. Wood, Infinite dilution partial molar properties of aqueous solutions of nonelectrolytes. I. Equations for partial molar volumes at infinite dilution and standard thermodynamic functions of hydration of volatile nonelectrolytes over wide ranges of conditions, Geochem. Cosmochim. Acta 64 (3) (2000) 495–512. https://doi.org/10.1016/S0016-7037(99)00322-1.
[19] F. Soubiran, B. Militzer, Miscibility calculations for water and hydrogen in giant planets, Astrophys. J. 806 (2015) 228. https://doi.org/10.1088/0004-637X/806/2/228.
[20] A.F. Goncharov, N. Goldman, L.E. Fried, J.C. Crowhurst, I.-F.W. Kuo, C.J. Mundy, J.M. Zaug, Dynamic ionization of water under extreme conditions, Phys. Rev. Lett. 94 (12) (2005) 125508. https://doi.org/10.1103/PhysRevLett.94.125508.
[21] W. Wagner, A. Saul, A. Pruß, International equations for the pressure along the melting and along the sublimation curve of ordinary water substance, J. Phys. Chem. Ref. Data 23 (3) (1994) 515–527. https://doi.org/10.1063/1.555947.
[22] J.G. Kirkwood, F.P. Buff, The statistical mechanical theory of solutions, J. Chem. Phys. 19 (6) (1951) 774–782. https://doi.org/10.1063/1.1748352.
[23] J.P. O'Connell, Thermodynamic properties of solutions based on correlation functions, Mol. Phys. 20 (1) (1971) 27–33. https://doi.org/10.1080/00268977100100031.
[24] J.M.H. Levelt Sengers, Solubility near the solvent's critical point, J. Supercrit. Fluids 4 (4) (1991) 215–222. https://doi.org/10.1016/0896-8446(91)90013-V.
[25] J.M.H. Levelt Sengers, Thermodynamics of solutions near the solvent's critical point, in: T.J. Bruno, J.F. Ely (Eds.), Supercritical Fluid Technology: Reviews in Modern Theory and Applications, CRC Press, Boca Raton, 1991, pp. 1–56.
[26] J. Alvarez, H.R. Corti, R. Fernández-Prini, M.L. Japas, Distribution of solutes between coexisting steam and water, Geochem. Cosmochim. Acta 58 (13) (1994) 2789–2798. https://doi.org/10.1016/0016-7037(94)90114-7.
[27] J.P. O'Connell, Application of fluctuation solution theory to thermodynamic properties of solutions, Fluid Phase Equilib. 104 (1995) 21–39.
[28] J.P. O'Connell, H. Liu, Thermodynamic modelling of near-critical solutions, Fluid Phase Equilib. 144 (1998) 1–12.
[29] A.V. Plyasunov, E.L. Shock, J.P. O'Connell, Corresponding-states correlations for estimating partial molar volumes of nonelectrolytes at infinite dilution in water over extended temperature and pressure ranges, Fluid Phase Equilib. 247 (1–2) (2006) 18–31. https://doi.org/10.1016/j.fluid.2006.06.007.
[30] B. Lee, Partial molar volume from the hard-sphere mixture model, J. Phys. Chem. 87 (1) (1983) 112–118. https://doi.org/10.1021/j100224a026.
[31] A.V. Plyasunov, Values of the Krichevskii parameter, A_{Kr}, of aqueous nonelectrolytes evaluated from relevant experimental data, J. Phys. Chem. Ref. Data 41 (3) (2012) 019901, 033104. (Erratum: J. Phys. Chem. Ref. Data 44 (2015), https://doi.org/10.1063/1.4748184.
[32] A.V. Plyasunov, Empirical evaluation of the Krichevskii parameter for aqueous solutes, J. Mol. Liq. 239 (2017) 92–95. https://doi.org/10.1016/j.molliq.2016.04.092.
[33] M.P. Hodges, R.J. Wheatley, A.H. Harvey, Intermolecular potential and second virial coefficient of the water–helium complex, J. Chem. Phys. 116 (4) (2002) 1397–1405. https://doi.org/10.1063/1.1421065.
[34] M.P. Hodges, R.J. Wheatley, A.H. Harvey, Intermolecular potentials and second virial coefficients of the water–neon and water–argon complexes, J. Chem. Phys. 117 (15) (2002) 7169–7179. https://doi.org/10.1063/1.1504703.
[35] M.P. Hodges, R.J. Wheatley, G.K. Schenter, A.H. Harvey, Intermolecular potential and second virial coefficient of the water–hydrogen complex, J. Chem. Phys. 120 (2) (2004) 710–720. https://doi.org/10.1063/1.1630960.
[36] O. Akin-Ojo, A.H. Harvey, K. Szalewicz, Methane-water cross second virial coefficient with quantum corrections from an ab initio potential, J. Chem. Phys. 125 (1) (2006) 014314. https://doi.org/10.1063/1.2207139.
[37] A.S. Tulegenov, M.P. Hodges, R.J. Wheatley, A.H. Harvey, Intermolecular potential and second virial coefficient of the water-nitrogen complex, J. Chem. Phys. 126 (9) (2007) 094305. https://doi.org/10.1063/1.2446843.
[38] R.J. Wheatley, A.H. Harvey, The water-oxygen dimer: first-principles calculation of an extrapolated potential energy surface and second virial coefficients, J. Chem. Phys. 127 (7) (2007) 074303. https://doi.org/10.1063/1.2756524.
[39] R.J. Wheatley, A.H. Harvey, Intermolecular potential energy surface and second virial coefficients for the nonrigid water-CO dimer, J. Chem. Phys. 131 (15) (2009) 154305. https://doi.org/10.1063/1.3244594.
[40] A.V. Plyasunov, E.L. Shock, R.H. Wood, Second cross virial coefficients for interactions involving water. Correlations and group contributions values, J. Chem. Eng. Data 48 (6) (2003) 1463–1470. https://doi.org/10.1021/je034047m.
[41] I. Kritchevsky, A. Iliinskaya, Partial molal volumes of gases dissolved in liquids (A contribution to the thermodynamics of dilute solutions of non-electrolytes), Acta Physicochim. URSS 20 (3) (1945) 327–348.
[42] W.L. Masterton, Partial molal volumes of hydrocarbons in water solution, J. Chem. Phys. 22 (11) (1964) 1830–1833. https://doi.org/10.1063/1.1739928.
[43] E.W. Tiepel, K.E. Gubbins, Partial molal volumes of gases dissolved in electrolyte solutions, J. Phys. Chem. 76 (21) (1972) 3044–3049. https://doi.org/10.1021/j100665a024.
[44] J.C. Moore, R. Battino, T.R. Rettich, Y.P. Handa, E. Wilhelm, Partial molar volumes of gases at infinite dilution in water at 298.15 K, J. Chem. Eng. Data 27 (1) (1982) 22–24. https://doi.org/10.1021/je00027a005.
[45] N. Bignell, Partial molar volumes of atmospheric gases in water, J. Phys. Chem. 88 (22) (1984) 5409–5412. https://doi.org/10.1021/j150666a060.
[46] H. Watanabe, K. Iizuka, The influence of dissolved gases on the density of water, Metrologia 21 (1) (1985) 19–26. https://doi.org/10.1088/0026-1394/21/1/005.
[47] L. Hnědkovský, R.H. Wood, V. Majer, Volumes of aqueous solutions of CH_4, CO_2, H_2S, and NH_3 at temperatures from 298.15 K to 705 K and pressures to 35 MPa, J. Chem. Thermodyn. 28 (2) (1996) 125–142. https://doi.org/10.1006/jcht.1996.0011.
[48] D.R. Biggerstaff, R.H. Wood, Apparent molar volumes of aqueous argon, ethylene, and xenon from 300 to 716 K, J. Phys. Chem. 92 (7) (1988) 1988–1994. https://doi.org/10.1021/j100318a056.
[49] T. Zhou, R. Battino, Partial molar volumes of 13 gases in water at 298.15 K and 303.15 K, J. Chem. Eng. Data 46 (2) (2001) 331–332. https://doi.org/10.1021/je000215o.
[50] J.M. Prausnitz, R.N. Lichtenthaler, E.G. de Avezedo, Molecular Thermodynamics of Fluid-phase Equilibria, third ed., Prentice-Hall, New York, 1999.
[51] B.E. Poling, J.M. Prausnitz, J.P. O'Connell, The Properties of Gases and Liquids, fifth ed., McGraw Hill, New York, 2001.
[52] E.L. Ratkova, M.V. Fedorov, On a relationship between molecular polarizability and partial molar volume in water, J. Chem. Phys. 135 (24) (2011) 244109. https://doi.org/10.1063/1.3672094.
[53] H.S. Ashbaugh, J.W. Barnett, N.d.S. Moura, H.E. Houser, Hydrated nonpolar solute volumes: interplay between size, attractiveness, and molecular structure, Biophys. Chem. 213 (2016) 1–5. https://doi.org/10.1016/j.bpc.2016.03.002.
[54] A. Bondi, van der Waals volumes and radii, J. Phys. Chem. 68 (3) (1964) 441–451.
[55] M. Mantina, A.C. Chamberlin, R. Valero, C.H. Cramer, D.G. Truhlar, Consistent van der Waals radii for the whole main group, J. Phys. Chem. A 113 (19) (2009) 5806–5812. https://doi.org/10.1021/jp8111556.
[56] A.V. Plyasunov, J.P. O'Connell, R.H. Wood, E.L. Shock, Infinite dilution partial molar properties of aqueous solutions of nonelectrolytes. II. Equations for the standard thermodynamic functions of hydration of volatile nonelectrolytes over wide ranges of conditions including subcritical temperatures, Geochem. Cosmochim. Acta 64 (16) (2000) 2779–2795. https://doi.org/10.1016/S0016-7037(00)00390-2.
[57] A.H. Harvey, Applications of near-critical dilute-solution thermodynamics, Ind. Eng. Chem. Res. 37 (8) (1998) 3080–3088. https://doi.org/10.1021/ie970800r.
[58] R. Fernández-Prini, J.L. Alvarez, A.H. Harvey, Henry's constants and vapor–liquid distribution constants for gaseous solutes in H_2O and D_2O at high temperatures, J. Phys. Chem. Ref. Data 32 (2) (2003) 903–916. https://doi.org/10.1063/1.1564818.
[59] M.L. Japas, J.M.H. Levelt Sengers, Gas solubility and Henry's law near the solvent's critical point, AIChE J. 35 (5) (1989) 705–713. https://doi.org/10.1002/aic.690350502.
[60] V.B. Polyakov, J. Horita, D.R. Cole, Isotopic self-exchange reactions of water: evaluation of the rule of the geometric mean in liquid-vapor isotope partitioning, J. Phys. Chem. A 109 (38) (2005) 8642–8645. https://doi.org/10.1021/jp053210c.
[61] A.V. Plyasunov, E.L. Shock, Prediction of the vapor-liquid distribution constants for volatile nonelectrolytes in water up to its critical temperature, Geochem. Cosmochim. Acta 67 (24) (2003) 4981–5009. https://doi.org/10.1016/j.gca.2003.08.003.
[62] E. Wilhelm, R. Battino, R.J. Wilcock, Low-pressure solubility of gases in liquid water, Chem. Rev. 77 (2) (1977) 219–262. https://doi.org/10.1021/cr60306a003.
[63] W. Wagner, A. Pruß, The IAPWS formulation for the thermodynamic properties of ordinary water substances for general and scientific use, J. Phys. Chem. Ref. Data 31 (2) (2002) 387–535. https://doi.org/10.1063/1.1461829.